

Exploring algorithms for quantum computing of atomic nuclei



INDIAN INSTITUTE OF TECHNOLOGY

Roorkee-247667, Uttarakhand, India

A Dissertation

Submitted to Department of Physics
In the Partial Fulfilment of the Requirements
For the Degree of Master of Science

by

Aman Gupta
20615004

Supervisor

Prof. P. Arumugam
Department of Physics



INDIAN INSTITUTE OF TECHNOLOGY ROORKEE

CANDIDATE'S DECLARATION

I, **Aman Gupta**, hereby declare that the work presented in this dissertation entitled "**Exploring algorithms for quantum computing of atomic nuclei**" submitted in the Department of Physics, Indian Institute of Technology, Roorkee, India in partial fulfilment for the award of the degree of Master of Science in Physics is an authentic record of my own work carried out during June 2021 to April 2022 under the supervision of the **Prof. P. Arumugam**, Department of Physics, Indian Institute of Technology, Roorkee

I have not submitted the material included in this dissertation for the award of any other degree from this or any other university.

Aman Gupta

CERTIFICATION

This is to certify that the candidate's above statement is correct to the best of my knowledge.

Prof. P. Arumugam
Department of Physics
Indian Institute of Technology, Roorkee

ACKNOWLEDGEMENT

I would like to thank my guide, professors, and friends at IIT Roorkee for their help and my parents for their support.

I am especially thankful to people without whose help this project would not have been possible to accomplish. First and foremost, I am grateful to Prof. P. Arumugam, my project supervisor and Dr. Pooja Siwach who have guided me at every step of this project. I want to express my heartfelt gratitude to them for devoting their time and attention to me during my work.

I would also like to express my love and gratitude to Abhishek Sharma, Nifeeya Singh and Ashutosh Singh, Ph.D. scholars, and my friends Devesh Kumar and Ateesh Singh for their unwavering support, insights and generous support during this project.

Finally, I want express my sincere gratitude to my family.

Aman Gupta
Department of Physics
Indian Institute of Technology, Roorkee
May, 2022

ABSTRACT

Quantum Computation techniques have been used to solve the Deuteron problem namely to obtain the eigenstates and eigenvalues of the groundstate of Deuteron. 2 encoding schemes(JWT and GC) are discussed to convert the Hamiltonian into sum weighted Pauli matrices. 3 quantum algorithms(VQE, QPE and DPE) are explored to obtain the desired properties. Modified QPE was also introduced to obtain the eigenstate by performing adiabatic time evolution of a guess state. These are algorithms are created such that it can be used to any nuclear many-body physics problems.

Contents

1	INTRODUCTION	1
2	INTRODUCTION TO QUANTUM COMPUTATION	2
3	NUCLEAR PHYSICS TO QUANTUM COMPUTATION PROBLEM	4
3.1	The Nuclear Hamiltonian	4
3.2	Encoding Schemes	5
3.2.1	Jordan-Wigner Transformation(JWT)	5
3.2.2	Gray Code Encoding(GC)	6
4	THE DEUTERON PROBLEM	8
4.1	For EFT Potential	8
4.2	For Central Potential	9
5	FORMALISM : QUANTUM ALGORITHMS	10
5.1	Variational Quantum Eigensolver(VQE)	10
5.1.1	Results for VQE	12
5.1.2	Discussions and Comments	13
5.2	Quantum Phase Estimation	14
5.2.1	Quantum Fourier Transform(QFT)	14
5.2.2	QPE Algorithm	15
5.2.3	Trotter-Suzuki Approximation	16
5.2.4	Choice of time interval	17
5.2.5	Choice of number of ancilla qubits	17
5.2.6	Iterative QPE	19
5.2.7	Excited states in QPE	19
5.2.8	Modified QPE	19
5.2.9	Results for QPE and modified QPE	21
5.2.10	Discussions and Comments	23
5.3	Direct Phase Estimation	24
5.3.1	Results for Direct Phase Estimation	26
5.3.2	Discussions and Comments	26
6	CONCLUSION	29

List of Figures

Figure 1	Qubit represented on a Bloch sphere, one qubit(a), multiple qubits(b)	2
Figure 2	An example of a Quantum Circuit	3
Figure 3	Flowchart for VQE algorithm	11
Figure 4	A general circuit for Quantum Fourier Transform. . . .	15
Figure 5	The 1 st stage of the phase estimation procedure. Normalization factors of 1/2 have been omitted, on the right.	16
Figure 6	A general circuit for Quantum Phase Estimation with c ancilla qubits.	17
Figure 7	Improvement in the accuracy of energy eigenvalue measurement with the increase in number of ancilla qubits using QPE algorithm	18
Figure 8	Quantum Circuit for iterative QPE	19
Figure 9	A flowchart of process to obtain eigenstate of system .	20
Figure 10	<i>Ansatz</i> for convergence, JWT, $N=(2(a), 3(b), 4(c))$, GC, $N= 2(d)$, respectively	21
Figure 11	Convergence of state to eigenstate with iterations with different number of ancilla qubits for JWT(a) and GC(b). .	22
Figure 12	State Fidelity between output state and eigenstate(top) with each iteration and number of ancilla qubits = 2 and the corresponding convergence of binding energies (bottom)	23
Figure 13	A generalised Quantum Circuit for Direct Phase Estimation	26
Figure 14	Comparison between QPE and DPE results, for EFT Potential (a) and Central Potential (b)	27

List of Tables

Table 1	Weighted Pauli Representation of Deuteron Hamiltonian with EFT Potential truncated to different basis sizes. Here the coefficients are the h_{ij} terms in Eq.(1) obtain classically and Pauli operators will be evaluated using quantum algorithms	8
Table 2	Same as Table 1 but with central potential	9
Table 3	VQE results for ground-state energy eigen value (MeV) with chosen <i>Ansatz</i>	12
Table 4	A comparison of effect of different <i>Ansatz</i> and classical optimizer for VQE	13
Table 5	Energy (in MeV) calculated with 'qasm simulator' using EFT potential for different number of basis states N and encodings. The results from exact diagonalization using classical numerical techniques are termed as 'true value'. For a larger N , the results from exact diagonalization get closer to the experimental value -2.226 MeV	24
Table 6	Same as Table 5 but with Central Potential	24

INTRODUCTION

Classical Computers are not very good at simulating the behaviours of a quantum system, quantum computers can. Also quantum many body problems are NP-Hard[1], therefore simulating them on a classical computer is not an easy, we need exponential speed of a quantum computer. This fact led to development of quantum computers and a surge in studies of quantum systems(such as Atoms and Molecules and their interactions) and classical systems using a quantum computer began. Application of Quantum Computer in Atomic and Molecular physics prove to be a great success and its application in nuclear physics has also great potential.

Most famous algorithms to simulate atomic and molecular system to obtain observables and the related state of the system are the Variational Quantum Eigensolver, Quantum Phase Estimation, Direct Phase Estimation(nth order), Direct Measurement of Hamiltonian and new and improved algorithms pop-up everyday. However these algorithms cannot be directly used for a nuclear many body problem, as, nuclear physics problems are described via quantum field theory on continuous spacetime, possible with infinite dimensional degrees of freedom per volume, and they should be encoded efficiently into an finite number of qubits on lattice and the underling theory for nuclear physics should respect gauge invariance, and in the corresponding quantum simulation, a physical Hilbert space should be kept.[2]

In Chapter 2, we briefly discuss the concepts and tools in Quantum Computation like qubits, quantum gates and circuits and how to use it in relevance to our problem. In next chapter we introduce our problem and discuss methods to convert a nuclear physics problem into a quantum computing problem, that is, we introduce encoding schemes like Jordan Wigner Transformation(JWT) and Gray Code(GC) encoding to transform our operators from Second Quantization[3] in Harmonic Oscillator basis into linear combination of Pauli operators and also difficulties to implement nuclear physics problems onto a quantum computer. In next chapter we take an example of a simple nuclear system, a Deuteron(with different nuclear potentials) and convert it into quantum computation problem with the transformation schemes discussed in previous chapter. In chapter 5 we introduce 3 algorithms (Variational Quantum Eigensolver, Quantum Phase Estimation and Direct Phase Estimation) with reference to the Deuteron Hamiltonian. Chapter 6 concludes with some ideas for future.

INTRODUCTION TO QUANTUM COMPUTATION

Quantum Computation very much similar classical computation with some different properties, for instance in classical computation the fundamental unit of information being carried by bits which has a state space of just two binary values '0' and '1', similarly in quantum computation the fundamental units of information are carried by qubits, each qubit is a 2 dimensional Hilbert space, qubits being a quantum mechanical objects can stay even in a superposition of the two states. A qubit state can be visualized on a Bloch sphere as in Fig.1. A qubit can in any state (all points on the surface of the sphere) available on the Bloch sphere. If the choice of basis states are $|0\rangle = \begin{pmatrix} 1 \\ 0 \end{pmatrix}$ and $|1\rangle = \begin{pmatrix} 0 \\ 1 \end{pmatrix}$, then the state represented Fig. 1(a) can be written as $|\psi\rangle = \frac{1}{\sqrt{2}}(|0\rangle + e^{i\pi/2}|1\rangle)$, a general state can be written as $|\psi\rangle = a|0\rangle + b|1\rangle$. If there multiple qubits describing the system then the combined state of the system is written as $|\Psi\rangle = |\psi_1\rangle \otimes |\psi_2\rangle \otimes \dots$, where $|\psi_i\rangle$ are individual system states.[4]

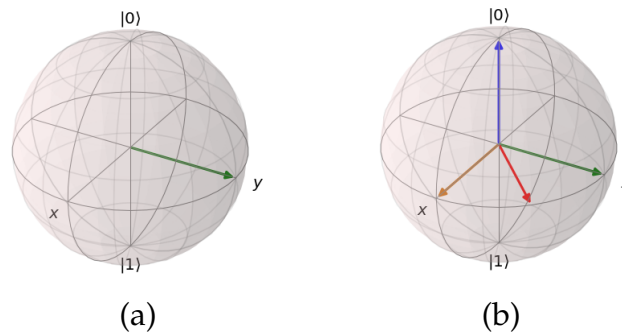


Figure 1: Qubit represented on a Bloch sphere, one qubit(a), multiple qubits(b)

The evolution of bits are governed by logical operators like OR, AND and XOR gates and the evolution of qubits are carried out by unitary operators called gates. These operators preserve the norm of the state. Some of the gates that we frequently used are:

Pauli Spin Matrices: $X = \begin{bmatrix} 0 & 1 \\ 1 & 0 \end{bmatrix}; Y = \begin{bmatrix} 0 & -i \\ i & 0 \end{bmatrix}; Z = \begin{bmatrix} 1 & 0 \\ 0 & -1 \end{bmatrix}$

Hadamard Gate : $H = \frac{1}{\sqrt{2}} \begin{bmatrix} 1 & 1 \\ 1 & -1 \end{bmatrix}$

Rotation Gates : $R_x(2\theta) = \begin{bmatrix} \cos \theta & -i \sin \theta \\ -i \sin \theta & \cos \theta \end{bmatrix}; R_y(2\theta) = \begin{bmatrix} \cos \theta & -\sin \theta \\ \sin \theta & \cos \theta \end{bmatrix};$

$R_z(2\theta) = \begin{bmatrix} e^{-i\theta} & 0 \\ 0 & e^{i\theta} \end{bmatrix}$

A quantum algorithm that we use are some sets of quantum operations on the qubits followed by measurement, represented by a quantum circuit(Fig. 2), and then some post-processing of the measurement results.

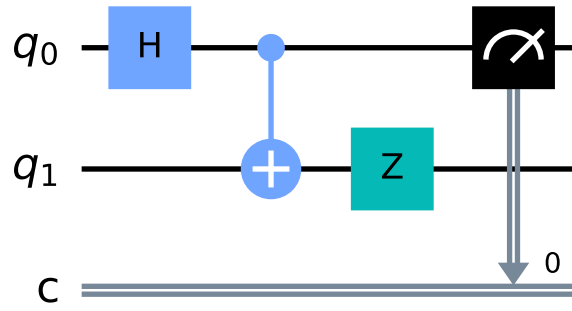


Figure 2: An example of a Quantum Circuit

We have used IBM's Qiskit(version : 0.19.1) platform to implement all the Quantum Computation algorithms used in this project.

NUCLEAR PHYSICS TO QUANTUM COMPUTATION PROBLEM

3.1 THE NUCLEAR HAMILTONIAN

In this project we simulated Hamiltonian H written in second quantization form as :

$$H = \sum_{ij} h_{ij} a_i^\dagger a_j, \quad (1)$$

where $h_{ij} = \langle i | \hat{T} + \hat{V} | j \rangle$. h_{ij} are calculated classically while $a_i^\dagger a_j$ are evaluated using quantum algorithms. The Hamiltonian for a simple nuclear system can be broken into two parts the Kinetic energy terms and the potential terms. When written in Harmonic Oscillator Basis, the Kinetic Energy operator is given by:

$$\langle n'l' | \hat{T} | nl \rangle = \frac{\hbar\omega}{2} \left[\left(2n + l + \frac{3}{2} \right) \delta_n^{n'} - \sqrt{n \left(n + l + \frac{1}{2} \right)} \delta_n^{n'+1} - \sqrt{(n+1) \left(n + l + \frac{3}{2} \right)} \delta_n^{n'-1} \right] \delta_l^{l'} \quad (2)$$

where $n(n') = 0, \dots, N-1$ is the radial quantum number of the harmonic oscillator basis with N determining the size of the basis, and $l(l')$ is the orbital angular momentum. For the case of the deuteron with $l = 0$ (3S_1 state), Eq.(2) becomes

$$\langle n'l' | \hat{T} | nl \rangle = \frac{\hbar\omega}{2} \left[\left(2n + \frac{3}{2} \right) \delta_n^{n'} - \sqrt{n \left(n + \frac{1}{2} \right)} \delta_n^{n'+1} - \sqrt{(n+1) \left(n + \frac{3}{2} \right)} \delta_n^{n'-1} \right] \quad (3)$$

The matrix element of potential terms for a Nuclear Hamiltonian depends upon the choice of potential, and for this project we consider 2 different forms of potentials.

1. **EFT Potential :** The matrix element for EFT potential is given by[5],[6] $\langle n'l' | V | n \rangle = V_0 \delta_n^{n'} \delta_n^0$, where the choice of coefficient $V_0 = -5.68658111$ MeV .

2. **Central Potential :** In the case of the EFT potential, the only nonzero matrix element corresponds to $n = 0$. It simplifies the problem to solve a tridiagonal operator. When the potential energy operator has nonzero off-tridiagonal matrix elements, the simulations can become complicated, leading to a greater number of terms in measurements. There are many different forms of central potential[7] but we will use

$$V(r) = 199.65e^{-\alpha_1 r^2} - 178.1e^{-\alpha_2 r^2},$$

to compute the binding energy of Deuteron. Here $\alpha_1 = 1.487 \text{ fm}^{-2}$ and $\alpha_2 = 0.639 \text{ fm}^{-2}$.

3.2 ENCODING SCHEMES

3.2.1 *Jordan-Wigner Transformation(JWT)*

This encoding scheme utilises only a small subspace of qubit's Hilbert space [8]. The number of qubits is equal to the number of occupation space available to the system. For example, for occupational number 4 (4 qubits) and 2 particles located at positions 1st and 2nd the state in occupational basis is represented by $|1100\rangle$, in qubits we therefore have 4 possible spin orbitals, 1 may be mapped to spin up orientation of qubit and so 0 to spin down. Mapping schema from occupation space to orientation of qubits is

$$\begin{aligned} \text{Occupation} &\longrightarrow \text{Qubit orientation} \\ \text{Ex.: } |1100\rangle &\longrightarrow |\uparrow\uparrow\downarrow\downarrow\rangle \\ \hat{a}_j &\longrightarrow \sigma_j^{(-)} \\ \hat{a}_j^\dagger &\longrightarrow \sigma_j^{(+)}, \end{aligned}$$

by defining the raising((+)) and lowering((-)) operators as

$$\begin{aligned} \sigma^{(+)} &= \frac{1}{2}(X - iY) = \begin{bmatrix} 0 & 0 \\ 1 & 0 \end{bmatrix} \\ \sigma^{(-)} &= \frac{1}{2}(X + iY) = \begin{bmatrix} 0 & 1 \\ 0 & 0 \end{bmatrix}, \end{aligned}$$

where X and Y are Pauli matrices. But for a fermionic creation and annihilation we also have to account for the change in sign and therefore we operate

with Pauli Z on all the qubits that come before j . So for an n qubit system the operation of \hat{a}_j and \hat{a}_j^\dagger acting on j^{th} qubit is:

3.2.1.1 JWT with Parity correction

$$\begin{aligned}\hat{a}_j &\longrightarrow \sigma_j^{(-)} \otimes Z_{j-1} \otimes Z_{j-2} \cdots \otimes Z_1, \\ \hat{a}_j^\dagger &\longrightarrow \sigma_j^{(+)} \otimes Z_{j-1} \otimes Z_{j-2} \cdots \otimes Z_1, \\ H &\longrightarrow H_q = \sum_{i\alpha} h_i \sigma_i^{(\alpha)} + \sum_{ij\alpha\beta} h_{ij} \sigma_i^{(\alpha)} \sigma_j^{(\beta)} + \cdots,\end{aligned}$$

In, H_q , the qubit Hamiltonian h_i and h_{ij} terms are obtained using classical computation methods while the Pauli terms operations are simulated using quantum algorithms.

3.2.2 Gray Code Encoding(GC)

Gray Code encoding scheme utilizes full Hilbert space of qubit basis, and hence reduces the number of qubits required exponentially[8]. A Gray code is an encoding of numbers so that adjacent numbers have a single digit differing by 1[9]. One choice of mapping the states to qubits would be the decimal representation of consecutive states[9]. Since the essence of Gray code encoding is in the Hamming distance, the creation and annihilation operators cannot be straightforwardly transformed to the qubit operations individually[8]. A choice for creation and annihilation operator transformation can be given by

$$\begin{aligned}a_i^\dagger a_j + a_j^\dagger a_i &= \prod_{\alpha \in T(i,j)} P_\alpha^{(i,\alpha)} \left(\prod_{\beta \in S(i,j)} Q_\beta^{(i,\beta)} + \prod_{\beta \in S(i,j)} Q_\beta^{(j,\beta)} \right) \\ &\quad \times [1 + \delta_{i,j}],\end{aligned}\tag{1}$$

where,

$$\begin{aligned}P_\alpha^{(0)} &= \frac{1}{2}(1 + Z_\alpha), P_\alpha^{(1)} = \frac{1}{2}(1 - Z_\alpha), \\ Q_\beta^{(0)} &= \frac{1}{2}(X_\beta + iY_\beta), Q_\beta^{(1)} = \frac{1}{2}(X_\beta - iY_\beta),\end{aligned}$$

and, $T(i, j)$ and $S(i, j)$ are set involving matching and mismatching qubits respectively.

For Example : For the Hamiltonian in, Eq.(1) the matrix element $\langle 00|H|01 \rangle =$

$\langle 00|(a_0^\dagger a_1 + a_1^\dagger a_0)|01\rangle$, matching qubits in $(00,01)$ is $\{1\}$ and mismatching qubits $\{0\}$ so $T(00,01) = \{1\}$ and $S(00,01) = \{0\}$, therefore the operator sandwiched between qubits in Gray code encoding transforms to

$$\begin{aligned}
 a_0^\dagger a_1 + a_1^\dagger a_0 &= \prod_{\alpha \in_1} P_\alpha^{(0,\alpha)} \left(\prod_{\beta \in_0} Q_\beta^{(0,\beta)} + \prod_{\beta \in_1} Q_\beta^{(1,\beta)} \right) [1 + \delta_{0,1}] \\
 &= P_1^{(0)} \left(Q_0^{(0)} + Q_0^{(1)} \right) \\
 &= X_0 P_1^{(0)} = \frac{1}{2} (X_0 + X_0 Z_1),
 \end{aligned} \tag{2}$$

THE DEUTERON PROBLEM

We use EFT potential and central potential to obtain the Deuteron Hamiltonian in sum weighted Pauli matrices representation.

4.1 FOR EFT POTENTIAL

Table 1: Weighted Pauli Representation of Deuteron Hamiltonian with EFT Potential truncated to different basis sizes. Here the coefficients are the h_{ij} terms in Eq.(1) obtain classically and Pauli operators will be evaluated using quantum algorithms

EFT Potential			
Case	Basis Size ↓	Jordan Wigner Transformation	Gray Code Encoding
1.1	$N = 2$	$H_2 = 5.9067091I + 0.218291Z_0 - 6.125Z_1 - 2.143304(X_0X_1 + Y_0Y_1)$	$H_2 = 5.9067091I - 6.34329Z_0 - 4.28661X_0$
1.2	$N = 3$	$H_3 = H_2 + 9.625(I - Z_2) - 3.91312(X_1X_2 + Y_1Y_2)$	$H_3 = 7.765855I - 7.984145Z_0 - 1.859145Z_1 + 1.640855Z_0Z_1 - 2.143305(X_0 + X_0Z_1) - 3.91312(X_1 - Z_0X_1)$
1.3	$N = 4$	$H_4 = 28.657I + 0.218Z_0 - 6.125Z_1 - 9.625Z_2 - 13.125Z_3 - 2.143X_0X_1 - 3.913X_1X_2 - 5.671X_2X_3 - 2.143Y_0Y_1 - 3.913Y_1Y_2 - 5.671Y_2Y_3$	$H_4 = 14.328I - 7.814X_0 - 3.913X_1 - 1.422Z_0 - 8.422Z_1 + 3.527X_0Z_1 + 3.913Z_0X_1 - 4.922Z_0Z_1$

4.2 FOR CENTRAL POTENTIAL

Table 2: Same as Table 1 but with central potential

Central Potential			
Case	Size of basis ↓	Jordan Wigner Transformation	Gray Code Encoding
2.1	$N = 2$	$H_2 = 7.858535I + 0.00257Z_0 - 7.861105Z_1 - 0.37778(X_0X_1 + Y_0Y_1)$	$H_2 = 7.858535I - 7.863675Z_0 - 0.75556X_0$
2.2	$N = 3$	$H_3 = H_2 + 15.92676(I - Z_2) - 3.6989(X_0Z_1X_2 + Y_0Z_1Y_2) + 4.123715(X_1X_2 + Y_1Y_2)$	$H_3 = 11.892645I - 11.895215Z_0 - 4.03411Z_1 + 4.03154Z_0Z_1 - 3.6989(X_0X_1 - Y_0Y_1) + 4.123715(X_1 - Z_0X_1) - 0.37778(X_0 + X_0Z_1)$

Now that we have the Hamiltonian in a weighted Pauli form, our challenge is to obtain information of our nuclear system, like its eigenstates, binding energy, resonance states and other observables using quantum algorithms. In upcoming chapters we have devised formalisms to obtain these features for Deuteron. We have come up with these formalisms in such a way that it can be applied to any other nuclear system or any quantum many-body problem as well. We also have described quantum algorithm that can be applied to a non-unitary, non-hermitian Hamiltonian which is not possible in classical computation.

5

FORMALISM : QUANTUM ALGORITHMS

In this chapter we discuss 3 quantum algorithms with reference to simulating a nuclear system with the example that we have chosen(see Chapter 3).

5.1 VARIATIONAL QUANTUM EIGENSOLVER(VQE)

VQE follows the variational principle of quantum mechanics where we have a parameterized wave-function(called *Ansatz*) and we then compute the expectation the value of ground-state energy for this wavefunction and then try to minimize this expectation value iteratively.

The VQE algorithm has 3 parts:

1. **State Preparation :** We have a state preparation circuit that prepares the parameterised state that is very close to the actual ground-state of the system.
2. **Ground-state Energy expectation value computation :** This part of the circuit computes the expectation energy value corresponding to the current state provided by the state preparation process.
3. **Classical Optimizer :** This process find the parameter that will minimize the expectation value. The process is iterative, i.e. it will every time choose a new parameter that will keep minimizing the energy expectation value, till it again starts increasing.

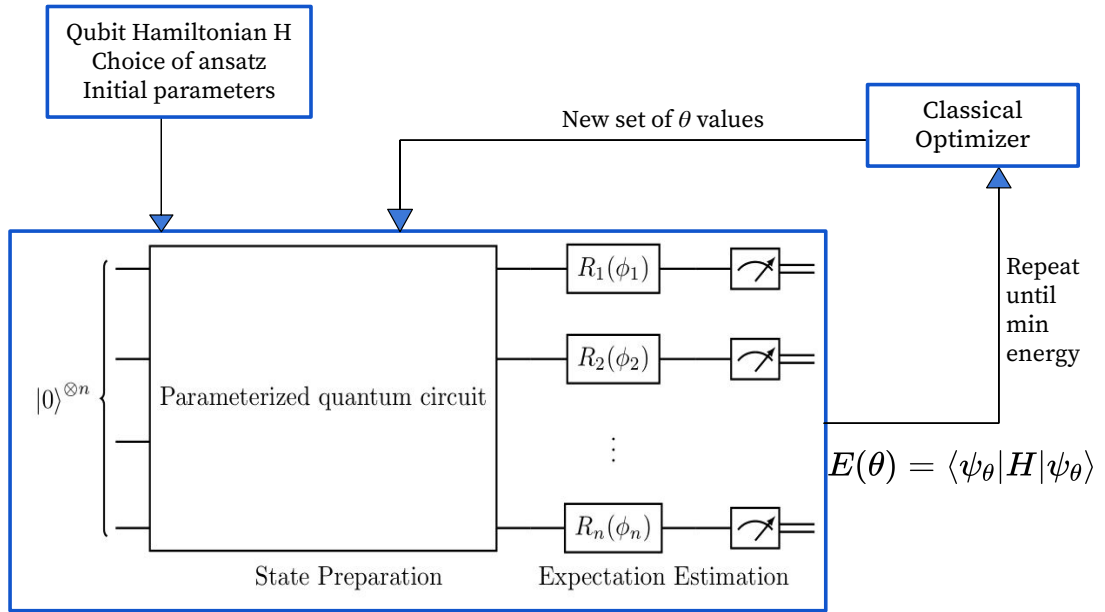
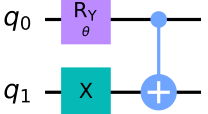
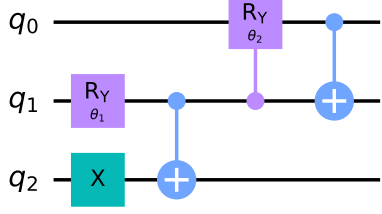
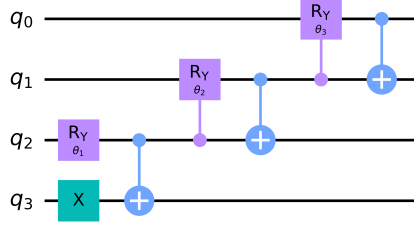


Figure 3: Flowchart for VQE algorithm

5.1.1 Results for VQE

The following results (Table 3) were obtained using IBM's simulator \rightarrow "qasm_simulator" and a classical optimizer "SPSA" on qiskit platform for (JWT) representation.

Table 3: VQE results for ground-state energy eigen value (MeV) with chosen *Ansatz*

Deuteron Hamiltonian(JWT)				
Size of Basis \downarrow	Ansatz used	Eigen Value Observed	Exact value (MeV)	Error
$N = 2$		-1.6227	-1.74916	0.12646
$N = 3$		-1.9816	-2.04567	0.06407
$N = 4$		-2.0199	-2.14308	0.12318

We also analysed the sensitivity of this algorithm with the choice of *Ansatz* and optimizer(see Table 4). The results for different *Ansatz* and classical optimizers for Cases 1.1 and 1.2, JWT in Table 1.

Table 4: A comparison of effect of different *Ansatz* and classical optimizer for VQE

<i>Ansatz</i>	Optimizer	Computed Value	Optimizer Time
<i>Ansatz, N = 2</i> (see Table 3)	COBYLA	−1.4607	2.6801
	L_BFGS_B	11.7029	5.2857
	SLSQP	12.9877	6.3572
	SPSA	−1.6227	19.8802
<i>Ansatz : Two_local</i> (qiskit's inbuilt)	COBYLA	−1.414	5.3062
	L_BFGS_B	12.0128	17.9021
	SLSQP	−0.3302	42.134
	SPSA	−0.8840	20.7937
<i>Ansatz</i>	Optimizer	Computed Value	Optimizer Time
<i>Ansatz, N = 3</i> (see Table 3)	COBYLA	−1.9537	5.06979
	L_BFGS_B	9.4717	8.7612
	SLSQP	−1.555	18.1123
	SPSA	−1.9816	21.6522
<i>Ansatz : Two_local</i> (qiskit's inbuilt)	COBYLA	−0.5706	10.9959
	L_BFGS_B	18.2131	44.7283
	SLSQP	8.3868	143.0192
	SPSA	−1.2322	22.8255

5.1.2 Discussions and Comments

From Table 4 we can draw following observations

1. The result is heavily depended on choice of optimizer and *Ansatz*, and for 'qasm_simulator' only 'COBYLA' and SPSA optimizers are good.
2. It produces a very accurate results with correct *Ansatz* and optimizer.
3. However it uses classical optimizer and hence prone to local optimizations(local minima). Ex: In case of 'L_BFGS_B' and 'SLSQP' optimizers.
4. VQE is very sensitive to choice of *Ansatz* and optimizer can give very different output values for different combination of the two.

5.2 QUANTUM PHASE ESTIMATION

Suppose a unitary operator U has an eigenvector $|u\rangle$ with eigenvalue $e^{2\pi i\theta}$, where the value of θ is unknown.

$$U|u\rangle = e^{2\pi i\theta}|u\rangle \quad (1)$$

The goal of the phase estimation algorithm is to estimate θ [10]. We can immediately relate this to unitary evolution operator of a system in Schrodinger's picture, if $H|\psi\rangle = E|\psi\rangle$ defines a system in state $|\psi\rangle$ with eigenvalue E , then its dynamics is written as

$$U|\psi\rangle = e^{-iEt}|\psi\rangle \quad (2)$$

. If we compare this to Eq. (1) the energy eigenvalue E relates to phase θ as

$$E = \frac{-2\pi\theta}{t}, \quad (3)$$

Before visiting the actual algorithm we introduce a very much required tool, Quantum Fourier Transform(QFT).

5.2.1 Quantum Fourier Transform(QFT)

QFT is essentially transformation of a qubit state from computational basis to fourier basis and the transformation for n qubits($N = 2^n$) is defined as:

$$|\tilde{x}\rangle \equiv QFT|x\rangle = \frac{1}{\sqrt{N}} \sum_{y=0}^{N-1} e^{2\pi i \frac{xy}{N}} |y\rangle \quad (4)$$

$|\tilde{x}\rangle$ is in fourier basis, $|x\rangle$ is in computational basis and $|y\rangle = |y_1 y_2 \dots y_n\rangle$ is in binary while y in summation is its decimal equivalent. Ex: if $|y\rangle = 4 \implies |y\rangle = |00 \dots 0100\rangle$ Expanding Eq. (4) we can write :

$$\begin{aligned} |\tilde{x}\rangle = \frac{1}{\sqrt{2}} \Big(& |0\rangle + e^{2\pi i x/2} |1\rangle \Big) \otimes \Big(|0\rangle + e^{2\pi i x/2^2} |1\rangle \Big) \\ & \otimes \dots \otimes \Big(|0\rangle + e^{2\pi i x/2^c} |1\rangle \Big) \end{aligned} \quad (5)$$

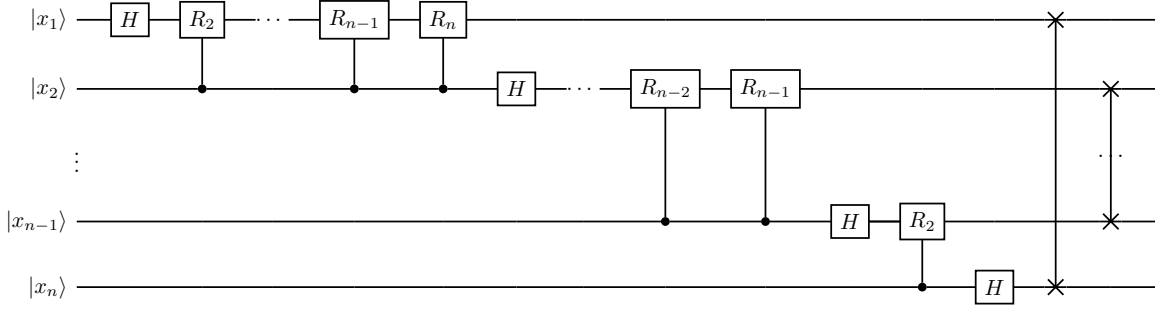


Figure 4: A general circuit for Quantum Fourier Transform.

so, effectively the individual states $|x\rangle = |x_1\rangle \otimes |x_2\rangle \otimes |x_3\rangle \otimes \cdots \otimes |x_c\rangle$ transform as:

$$\begin{aligned}
 |x_1\rangle &\longrightarrow (|0\rangle + e^{2\pi i x/2} |1\rangle) \\
 |x_2\rangle &\longrightarrow (|0\rangle + e^{2\pi i x/2^2} |1\rangle) \\
 |x_3\rangle &\longrightarrow (|0\rangle + e^{2\pi i x/2^3} |1\rangle) \\
 &\vdots \\
 |x_n\rangle &\longrightarrow (|0\rangle + e^{2\pi i x/2^c} |1\rangle)
 \end{aligned}$$

The circuit for a general QFT is represented by Fig. 4

5.2.2 QPE Algorithm

Quantum Phase Estimation Algorithm uses one ancilla register of c number of qubits that acts as control and one state register that stores the state of the system with however many qubits that it requires. c is decided by the degree of accuracy we want in estimating the phase and with what probability we wish the algorithm to succeed[10]. This algorithm is performed in two stages, in stage 1 we apply Hadamard to all qubits in ancilla register and then controlled U operations on state register with successive powers of two, demonstrated in Fig. 5:

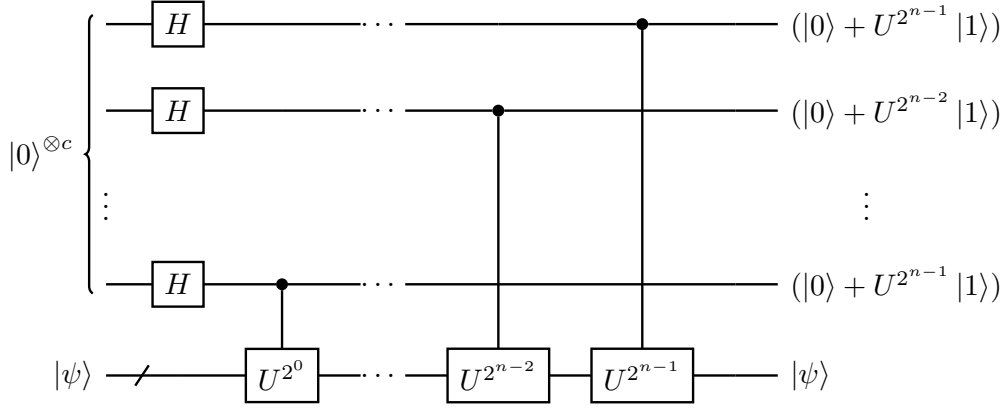


Figure 5: The 1st stage of the phase estimation procedure. Normalization factors of $1/2$ have been omitted, on the right.

The application of circuit in Fig. 5 results in the state of both registers as :

$$\begin{aligned}
 QPE|0\rangle^{\otimes c}|\psi\rangle &= \left(\frac{1}{\sqrt{2}}\right)^c (|0\rangle + e^{2\pi i\theta 2^{c-1}}|1\rangle) \\
 &\otimes (|0\rangle + e^{2\pi i\theta 2^{c-2}}|1\rangle) \otimes \dots \\
 &\otimes (|0\rangle + e^{2\pi i\theta 2^0}|1\rangle)|\psi\rangle,
 \end{aligned} \tag{6}$$

comparing this with Eq. (5) we see that action of both QPE and QFT circuit is same except $\theta \rightarrow \theta/2^c$. So by applying QFT inverse as the next stage and this transformation on θ we obtain θ .

We use modified QPE to 1st obtain the eigenstate of the system corresponding to the groundstate by performing adiabatic time evolution[11] of a state iteratively until it we obtain the actual groundstate. Next, we use QPE to obtain the energy eigenvalue with the final state obtained from previous step.

5.2.3 Trotter-Suzuki Approximation

For a Hamiltonian of form $H = \sum_{i=0}^L H_i$, the evolution operator is $U = e^{-iHt} = e^{-it\sum_{i=0}^L H_i} = e^{-itH_0}e^{-itH_1} \dots e^{-itH_L}$, i.e. we can apply each term individually if $[H_i, H_j] = 0 \forall i, j \in [0, L]$, i.e. all terms in Hamiltonian commute with each other. If all the terms in Hamiltonian do not commute then[12]

$U = e^{-iHt} \approx \prod_{i=0}^L \left[e^{-iH_i(t/N)} \right]^N$, where large N (will refer as trotter number from here onwards) means more accuracy.

Remark : Through my observations I have concluded that in our choice of

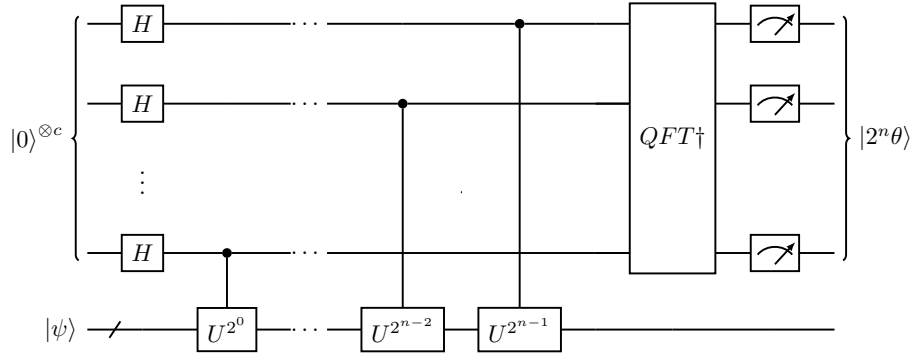


Figure 6: A general circuit for Quantum Phase Estimation with c ancilla qubits.

Hamiltonian if we have negative energy eigenvalues then Eq. (3) works but for we have positive eigenvalues we have to modify θ to $\theta \rightarrow 2^c - \theta$ and then use Eq. (3).

5.2.4 Choice of time interval

The choice of time interval t is very crucial to determine the spectrum of energy eigenvalues observed. To properly estimate all eigenvalues we take into account the periodicity of $e^{2\pi i \theta}$. If we want all the eigenvalues to lie in our spectrum, then θ should satisfy $0 \leq \theta \leq 1$, and since $\theta = -E\Delta t/2\pi$ (from Eq. (3)), $\theta = 0$ corresponds to minimum energy eigenvalue(E_{min}) of H and $\theta = 1$ corresponds to the maximum value(E_{max}). Therefore we can have maximum time interval to be

$$\max(\Delta t) = \frac{2\pi}{E_{max} - E_{min}} \quad (7)$$

5.2.5 Choice of number of ancilla qubits

The number of ancilla qubits dictates the ability to observe however many eigenvalues can be observed and also the accuracy of each measurement value[[13]]. For a given number of ancilla qubits say, c the largest number of distinct eigenvalues that can be observed is 2^c . Therefore the least number of ancilla qubits used should start from $\log_2(\dim(H))$, however if H has degeneracy then this least value can be reduced. The error in observing an eigenvalue is dependent

on ancilla qubits by[10],

$$t = c + \lceil \log \left(2 + \frac{1}{2\epsilon} \right) \rceil$$

ϵ is degree of error in measured eigenvalue to actual, t is total number of qubits(ancilla+system). Therefore, there is a trade-off between the amount of resource and the accuracy required. The best action, therefore for number of ancilla qubits is to start with absolute minimum required and then increase by one every-time while observing the gain in accuracy. We stop when increasing if ancilla qubits doesn't improve the result very much or stops improving altogether. We see that for almost all relevant cases the improvement in energy eigenvalue observation becomes very small beyond 8 ancilla qubits, see Fig. (7). Also another observation that made from same result is, the encoding scheme doesn't have an effect on the result.

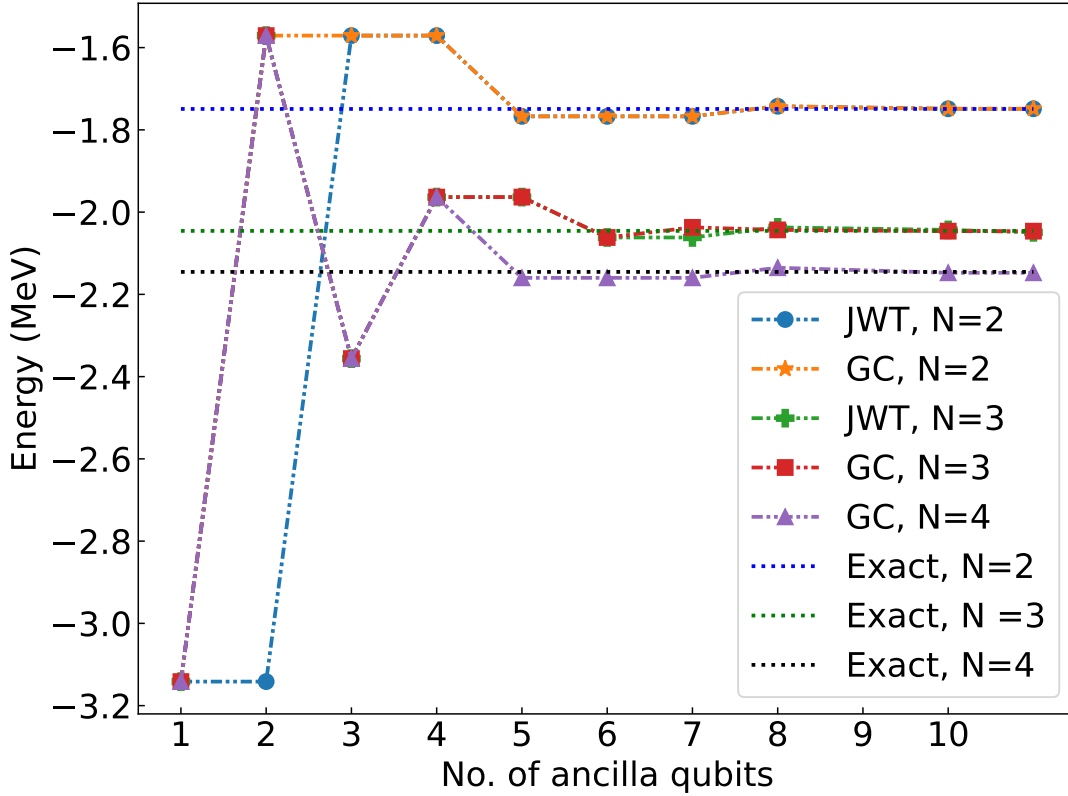


Figure 7: Improvement in the accuracy of energy eigenvalue measurement with the increase in number of ancilla qubits using QPE algorithm

5.2.6 Iterative QPE

As 5.2.5 discussed the number of ancilla qubits very much dictates the success of algorithm, it is also very much resource demanding, with each addition of new ancilla qubit the number of gates applied increases by 2^m (where m is number of gates with 1 less ancilla qubit). To avoid this, we can use a modified algorithm where we separate the circuit into c different circuits with only 1 ancilla qubit and perform QPE in iterative procedure. This approach is made possible by the semi-classical Quantum Fourier Transform[14] and is known as the Iterative Phase Estimation algorithm (IPEA)

In the IPEA, each digit of one $0.\theta_1\theta_2\cdots$ observation is estimated with a dedicated measurement using the circuits in Fig. (8). We iterate the circuit k times to obtain the value for θ_k and therefore improve the resolution for phase θ to greater accuracy.

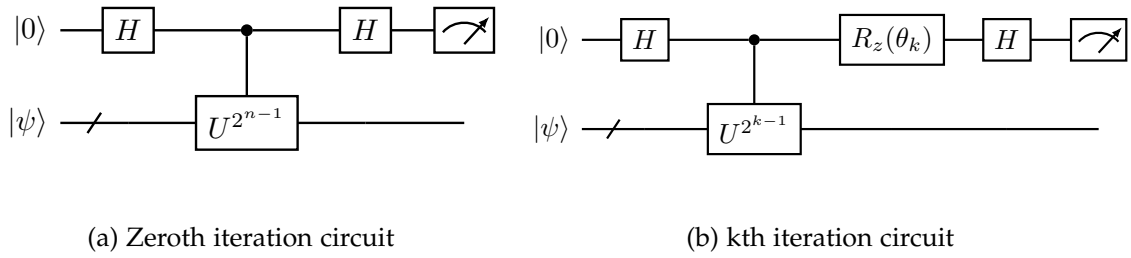


Figure 8: Quantum Circuit for iterative QPE

5.2.7 Excited states in QPE

To find the eigen-energy of the excited states of Deuteron represented in different basis sizes in Quantum Phase Estimation method, simply replace the ground state qubit representation to an excited state on the state register and perform the algorithm[15].

5.2.8 Modified QPE

We obtain eigenstate of a system by performing adiabatic time evolution on state register via modified QPE algorithm. The method is detailed in the flowchart 9.

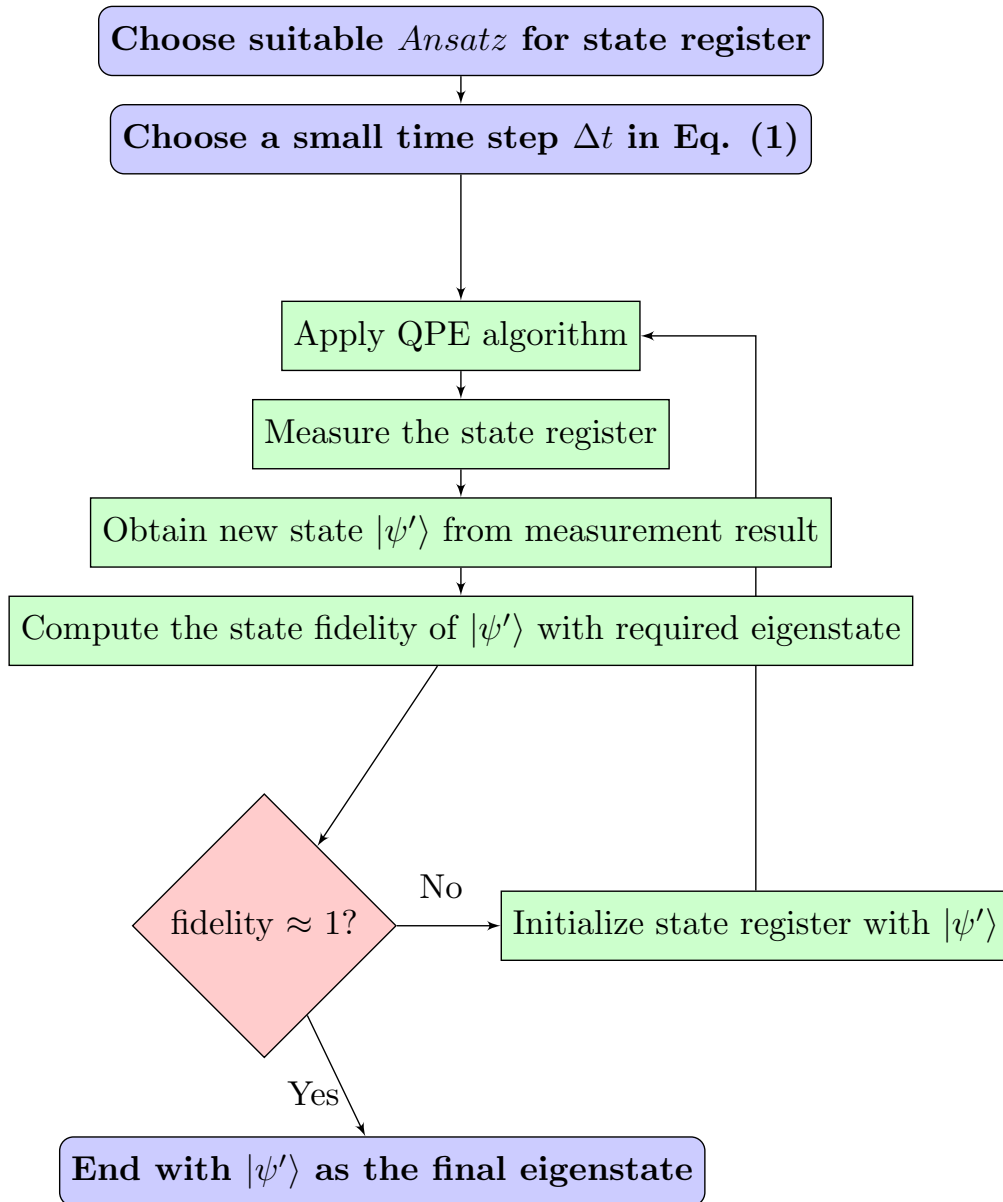


Figure 9: A flowchart of process to obtain eigenstate of system

Some *Ansatz* that we used are shown in Fig. 10

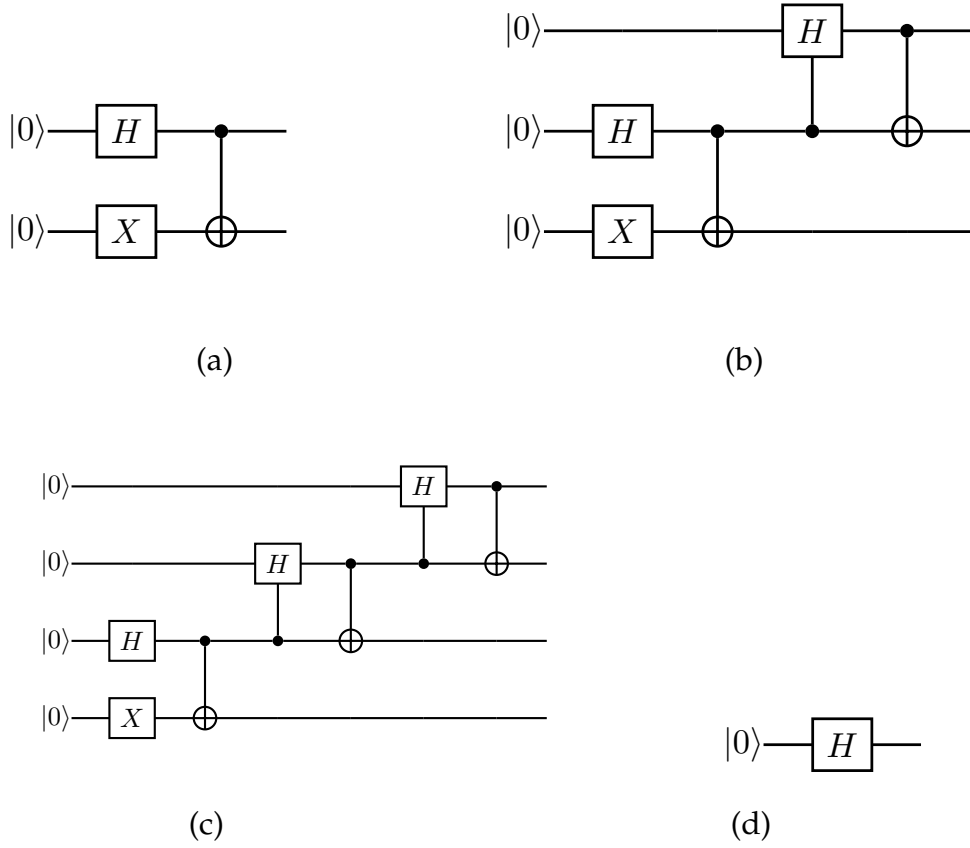


Figure 10: *Ansatz* for convergence, JWT, $N=2$ (a), 3(b), 4(c)), GC, $N=2$ (d), respectively

5.2.9 Results for QPE and modified QPE

We made an observation that modified QPE is independent to the choice of number of ancilla qubits as long as it is greater than 1, i.e. we can chose number of ancilla qubits to be 2 an still be able to obtain the eigenstate starting from *Ansatz*. In Fig. 11 we computed the state fidelity[16] of the state output with expected eigenstate to show that the state still evolved into an eigenstate by adiabatic time evolution for a range of ancilla qubits.

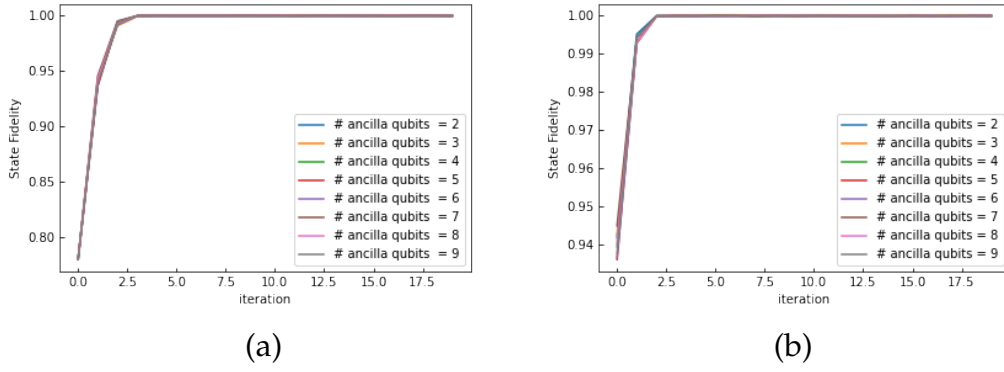


Figure 11: Convergence of state to eigenstate with iterations with different number of ancilla qubits for JWT(a) and GC(b).

We implemented modified QPE with 2 ancilla qubits to obtain the eigenstate and calculate the state fidelity of input state with eigenstate and also compute the convergence of energy eigenvalues using QPE at each iteration step (See Fig. 12).

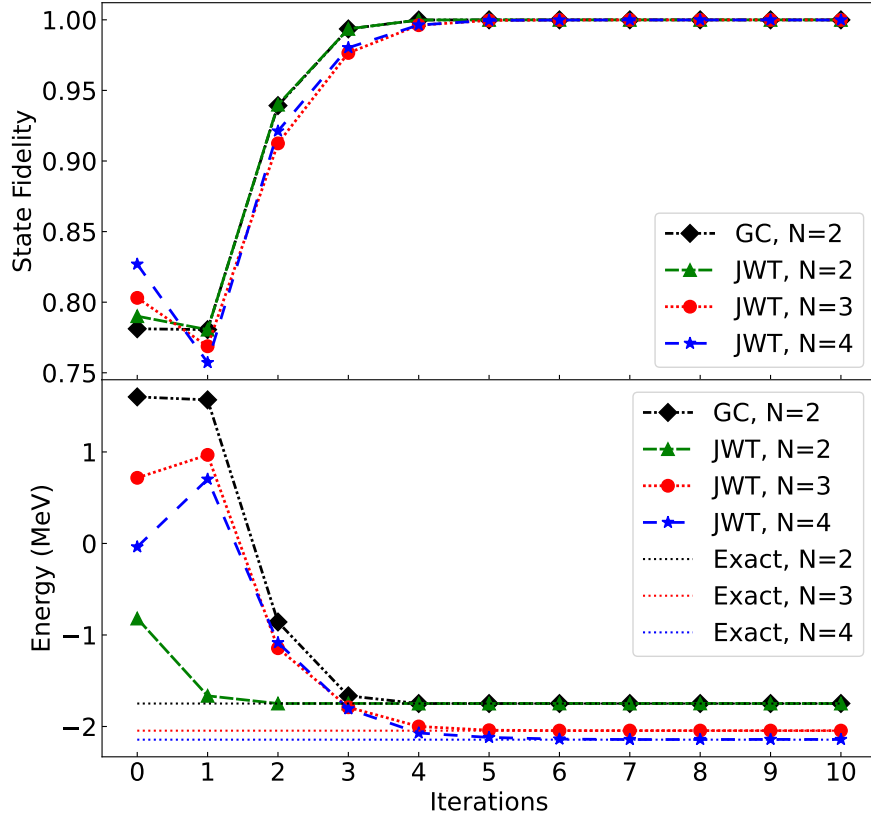


Figure 12: State Fidelity between output state and eigenstate(top) with each iteration and number of ancilla qubits = 2 and the corresponding convergence of binding energies (bottom)

We performed similar simulations of Hamiltonians mentioned in Tables 1 and 2 with QPE and to obtain groundstate and corresponding energy eigenvalue convergence of Deuteron in EFT and central potential shown in Fig. 12. The eigenvalue results as we see in Tables 5 and 6 are very close to the actual eigenvalue obtained by diagonalization.

5.2.10 Discussions and Comments

1. QPE and modified QPE are completely quantum algorithms with no classical parts unlike VQE and is therefore does get stuck in a local minima.

Table 5: Energy (in MeV) calculated with 'qasm simulator' using EFT potential for different number of basis states N and encodings. The results from exact diagonalization using classical numerical techniques are termed as 'true value'. For a larger N , the results from exact diagonalization get closer to the experimental value -2.226 MeV

Basis Size N	True Value	JWT	GC
2	-1.74916	-1.74874	-1.74874
3	-2.04567	-2.12302	-2.04326
4	-2.145	-2.14167	-2.14757

Table 6: Same as Table 5 but with Central Potential

Basis Size N	True Value	JWT	GC
2	-0.0413	-0.04295	-0.04295
3	-1.709	-1.73016	-1.70885
4	-1.739	-1.69352	-1.13515

2. QPE requires lots of resources in terms of qubits and gates and therefore the error in results for implementation on a NISQ era real quantum computer is very large.
3. However we have the scope to use iterative QPE on a real quantum computer and perform error mitigation at each iteration.
4. Modified QPE can be used in conjunction with any other algorithm to obtain the eigenstate of a system, it requires only 2 extra qubits (ancilla qubits), therefore is not resource heavy and it also can be implemented on a real device with error mitigation.

5.3 DIRECT PHASE ESTIMATION

Direct Phase Estimation algorithm is based on the method of Linear Combination of Unitaries(LCU)[17] to perform a sum of unitaries using a quantum circuit. With this algorithm we can implement any non-unitary operator with eigenvalues that has both real and imaginary parts, on quantum computer.

This is achieved by encoding the Hamiltonian into a bigger unitary operator. Suppose we have a nuclear Hamiltonian of form

$$H = \sum_{i=0}^{k-1} \alpha_i P_i \quad (1)$$

with complex energy eigen values and P_i are Pauli Operators, then we rewrite this Hamiltonian as

$$H = \sum_{i=0}^{2^n-1} \beta_i V_i \quad (2)$$

where $n = \lceil \log_2 k \rceil$ is number of qubits, β_i and unitary operator V_i are defined as :

$$\begin{aligned} \beta_i &= |\alpha_i|, V_i = \frac{\alpha_i}{|\alpha_i|} P_i, \text{ when } i < k \\ \beta_i &= 0, V_i = I, \text{ when } i \geq k \end{aligned} \quad (3)$$

We define an operator U to encode β_i s that satisfies the condition

$$U|0\rangle^{\otimes n} = \sum_j \gamma_j |j\rangle \quad (4)$$

where $\gamma_j = \sqrt{\frac{\beta_j}{A}}$, $A = \sum_j \beta_j$.

A generalized quantum circuit for DPE is given by Fig. 13. If the system is prepared in eigenstate $|\psi\rangle_s$ then the unitary action(U_r) of this circuit is

$$U_r|0\rangle_a|\psi\rangle_s = \frac{1}{A}|0\rangle_a U_r|\psi\rangle_s + |\Phi^\perp\rangle \quad (5)$$

$$= \frac{E}{A}|0\rangle_a|\psi\rangle_s + |\Phi^\perp\rangle \quad (6)$$

where $|\Phi^\perp\rangle$ is orthogonal to $|0\rangle_a|\psi\rangle_s$. Measurement on ancilla qubits multiple times gives a probability of measuring all os in ancilla qubits related to ground state energy eigenvalue the relation of which is given by

$$P(000..) = \frac{E^2}{A^2} \quad (7)$$

Using this algorithm we can also compute the imaginary part of energy eigenvalue by simply replacing H in Eq. (1) with $H' = (|E|/A)I + H$ and hence we have U' in Eq. (4) apply DPE. The result of implementing U' is

$$U'|0\rangle_a|\psi\rangle_s = \frac{|E|}{A}(1 + e^{i\theta})|0\rangle_a|\psi\rangle_s + |\Phi'^\perp\rangle \quad (8)$$

and so the measurement result in value $2(|E|/A)\cos\theta$ and with Eq. (7) we can obtain the complex part of energy eigenvalue. Therefore with this algorithm we can also obtain resonance states of any quantum system.

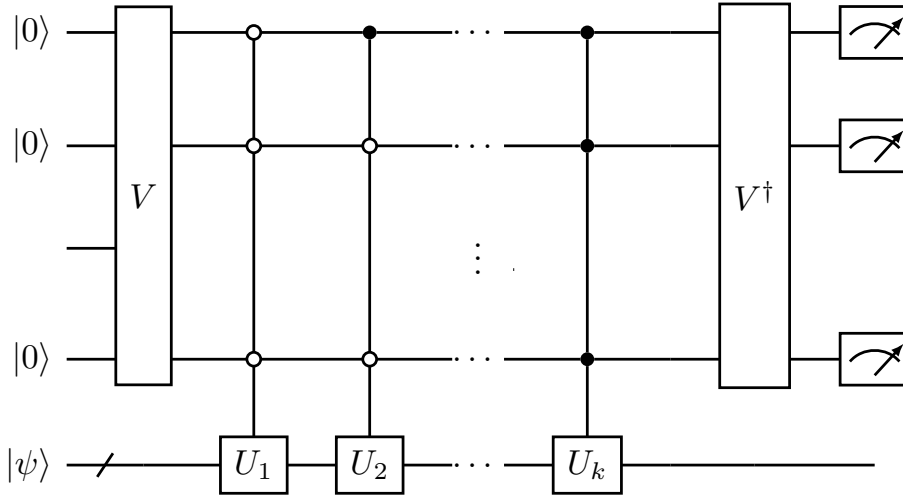


Figure 13: A generalised Quantum Circuit for Direct Phase Estimation

5.3.1 Results for Direct Phase Estimation

We implemented DPE algorithms and compared the results of energy eigenvalues obtained from QPE. We again used modified QPE to obtain the eigenstates and then DPE to obtain the energy eigenvalue. We implemented both with 20 different runs for each and from Fig. 14 we can see that DPE has error bars while QPE does as DPE computes energy eigenvalues with probability of observation of all zeros in the result while QPE uses the phase of max observation. Therefore with each run the results of DPE changes a little while QPE always gives the same result.

5.3.2 Discussions and Comments

1. DPE requires less resources than QPE as the number ancilla qubits doesn't scale with basis size.
2. DPE algorithm can be used to also compute resonances of a nuclear system.
3. However DPE relies on the square root of probability to compute eigenvalues of an observable hence has large variance with each new run of the experiment, while QPE uses the phase corresponding to maximum observation and hence produces same result with each run.

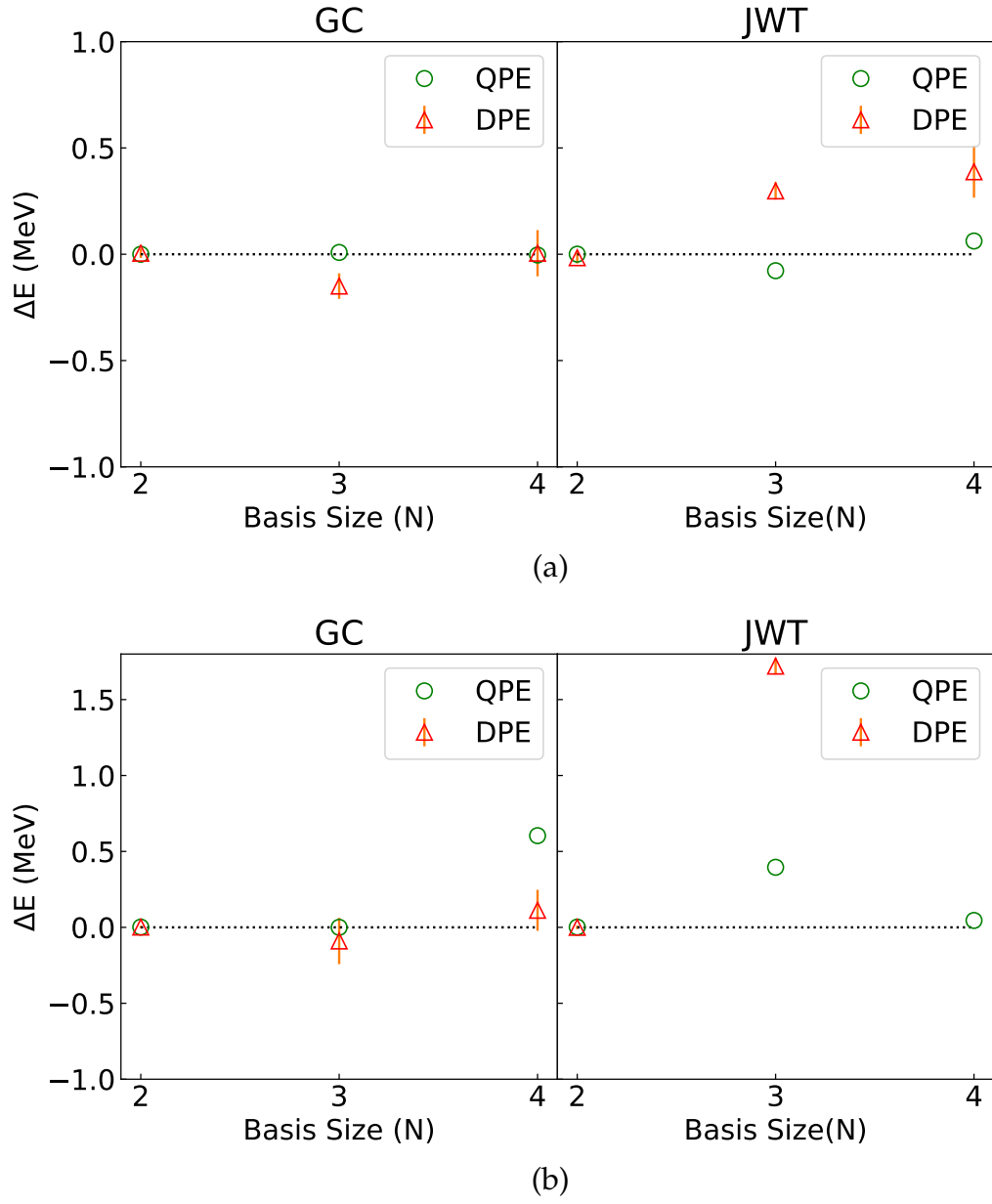


Figure 14: Comparison between QPE and DPE results, for EFT Potential (a) and Central Potential (b)

4. From Fig. 14 we see that QPE results are more accurate than DPE and we can further increase the accuracy by increasing the number of ancilla qubits and or trotter number, while in DPE we cannot do such a exercise to improve accuracy.

CONCLUSION

We have successfully used modified Quantum Phase Estimation Algorithm to find out the convergence of a non-parameterised *Ansatz* to an eigenstate and then obtained binding energy values for Deuteron in EFT and Central Potential truncated at different basis sizes, using QPE and DPE. Although the method is applied to a specific problem, these can be used in general to any many-body problems.

Quantum Algorithms are very useful and efficient in solving nuclear physics problems or any quantum mechanical problem even in NISQ era. The discussed algorithms QPE, modified QPE and DPE are implemented here on a simulator but implementation of DPE, modified QPE and iterative QPE are also possible on NISQ era quantum computers with some error mitigation techniques like Zero-noise Extrapolation and Probabilistic Error Correction. There are numerous other algorithms like Direct Measurement of Hamiltonian[18], Linear Combination of Unitaries[17], and Hadamard test, etc. that can be used to solve other aspects of any problem like obtaining resonance states, linear response, quadrupole moment etc. These are exactly the problems that we will be focusing in our future research.

Conferences and Publications

Conferences

- Gupta A., Siwach P., & Arumugam P. (2021). Exploring algorithms for quantum computing of atomic nuclei. In *Proceedings of the DAE Symp. on Nucl. Phys* (Vol. 65, p. 126).

Publications(In Submission Process)

- Gupta, A., Siwach, P., & Arumugam, P., Exploring Phase Estimation algorithms for quantum computing of atomic nuclei. In Submission Process.

Availability of Code and other resources

Github for Code and other resources

REFERENCES

1. Troyer, M. & Wiese, U.-J. Computational Complexity and Fundamental Limitations to Fermionic Quantum Monte Carlo Simulations. *Phys. Rev. Lett.* **94**, 170201. doi:[10.1103/PhysRevLett.94.170201](https://doi.org/10.1103/PhysRevLett.94.170201). <https://link.aps.org/doi/10.1103/PhysRevLett.94.170201> (17 May 2005).
2. Zhang, D.-B., Xing, H., Yan, H., Wang, E. & Zhu, S.-L. Selected topics of quantum computing for nuclear physics. *Chinese Physics B* **30**, 020306. doi:[10.1088/1674-1056/abd761](https://doi.org/10.1088/1674-1056/abd761). http://cpb.iphy.ac.cn/EN/abstract/article_123270.shtml (2021).
3. Hjorth-Jensen, M. *Second Quantization* July 2015. <http://nucleartalent.github.io/Course2ManyBodyMethods/doc/pub/secondquant/html/secondquant-bs.html>.
4. Nielsen, M. A. & Chuang, I. L. *Quantum Computation and Quantum Information: 10th Anniversary Edition* doi:[10.1017/CB09780511976667](https://doi.org/10.1017/CB09780511976667) (Cambridge University Press, 2010).
5. Dumitrescu, E. F. *et al.* Cloud Quantum Computing of an Atomic Nucleus. *Phys. Rev. Lett.* **120**, 210501. doi:[10.1103/PhysRevLett.120.210501](https://doi.org/10.1103/PhysRevLett.120.210501). <https://link.aps.org/doi/10.1103/PhysRevLett.120.210501> (21 May 2018).
6. Di Matteo, O. *et al.* Improving Hamiltonian encodings with the Gray code. *Phys. Rev. A* **103**, 042405. doi:[10.1103/PhysRevA.103.042405](https://doi.org/10.1103/PhysRevA.103.042405). <https://link.aps.org/doi/10.1103/PhysRevA.103.042405> (4 Apr. 2021).
7. Lecture Notes. *Frontiers in nuclear and hadronic physics*. <http://fnhp-school.mi.infn.it/lectures.html>.
8. Siwach, P. & Arumugam, P. Quantum simulation of nuclear Hamiltonian with a generalized transformation for Gray code encoding. *Phys. Rev. C* **104**, 034301. doi:[10.1103/PhysRevC.104.034301](https://doi.org/10.1103/PhysRevC.104.034301). <https://link.aps.org/doi/10.1103/PhysRevC.104.034301> (3 Sept. 2021).
9. Gray Code. *Wolfram MathWorld*. <https://mathworld.wolfram.com/GrayCode.html>.
10. Nielsen, M. A. & Chuang, I. L. *Chapter 5* (Cambridge University Press, 2017).
11. Farhi, E., Goldstone, J., Gutmann, S. & Sipser, M. Quantum Computation by Adiabatic Evolution. *arXiv: Quantum Physics* (2000).

12. Zhang, D.-B., Xing, H., Yan, H., Wang, E. & Zhu, S.-L. Selected topics of quantum computing for nuclear physics. *Chinese Physics B* **30**, 020306. doi:[10.1088/1674-1056/abd761](https://doi.org/10.1088/1674-1056/abd761). http://cpb.iphy.ac.cn/EN/abstract/article_123270.shtml (2021).
13. Ovrum, E. & Hjorth-Jensen, M. Quantum computation algorithm for many-body studies. *arXiv: Quantum Physics* (2007).
14. Griffiths, R. B. & Niu, C.-S. Semiclassical Fourier Transform for Quantum Computation. *Phys. Rev. Lett.* **76**, 3228–3231. doi:[10.1103/PhysRevLett.76.3228](https://doi.org/10.1103/PhysRevLett.76.3228). <https://link.aps.org/doi/10.1103/PhysRevLett.76.3228> (17 Apr. 1996).
15. Bian, T., Murphy, D., Xia, R., Daskin, A. & Kais, S. Quantum computing methods for electronic states of the water molecule. *Molecular Physics* **117**, 2069–2082. ISSN: 1362-3028. doi:[10.1080/00268976.2019.1580392](https://doi.org/10.1080/00268976.2019.1580392). <http://dx.doi.org/10.1080/00268976.2019.1580392> (Feb. 2019).
16. *Quantiki.org*. 2022. *Fidelity* <https://www.quantiki.org/wiki/fidelity>.
17. Childs, A. M. & Wiebe, N. Hamiltonian Simulation Using Linear Combinations of Unitary Operations. *Quantum Info. Comput.* **12**, 901–924. ISSN: 1533-7146 (Nov. 2012).
18. Bian, T., Murphy, D., Xia, R., Daskin, A. & Kais, S. Quantum computing methods for electronic states of the water molecule. *Molecular Physics* **117**, 2069–2082. doi:[10.1080/00268976.2019.1580392](https://doi.org/10.1080/00268976.2019.1580392). eprint: <https://doi.org/10.1080/00268976.2019.1580392>. <https://doi.org/10.1080/00268976.2019.1580392> (2019).

14%

SIMILARITY INDEX

7%

INTERNET SOURCES

11%

PUBLICATIONS

3%

STUDENT PAPERS

PRIMARY SOURCES

1	Pooja Siwach, P. Arumugam. "Quantum simulation of nuclear Hamiltonian with a generalized transformation for Gray code encoding", Physical Review C, 2021 Publication	5%
2	silo.pub Internet Source	1%
3	iopscience.iop.org Internet Source	1%
4	Submitted to Universiteit van Amsterdam Student Paper	1%
5	rua.ua.es Internet Source	1%
6	hdl.handle.net Internet Source	1%
7	digital.library.unt.edu Internet Source	1%
8	Sebastian Schröter, Paul-Antoine Hervieux, Giovanni Manfredi, Johannes Eiglsperger,	<1%

Javier Madroño. "Exact treatment of planar two-electron quantum dots: Effects of anharmonicity on the complexity", Physical Review B, 2013

Publication

9

Submitted to I-Shou International School

Student Paper

<1 %

10

arxiv.org

Internet Source

<1 %

11

Simran Jakhodia, Divyanshu Singh, Babita Jajodia. "Chapter 31 Experimental Evaluation of QFT Adders on IBM QX Hardware", Springer Science and Business Media LLC, 2022

Publication

<1 %

12

Teng Bian, Daniel Murphy, Rongxin Xia, Ammar Daskin, Sabre Kais. "Quantum computing methods for electronic states of the water molecule", Molecular Physics, 2019

Publication

<1 %

13

docplayer.net

Internet Source

<1 %

14

ntnuopen.ntnu.no

Internet Source

<1 %

15

Submitted to University of Warwick

Student Paper

<1 %

16	Submitted to London School of Economics and Political Science Student Paper	<1 %
17	lib.dr.iastate.edu Internet Source	<1 %
18	GRZEGORZ ŚWIATEK, EDSON VARGAS. "Decay of geometry in the cubic family", Ergodic Theory and Dynamical Systems, 1998 Publication	<1 %
19	Ri-Gui Zhou, Chen-Yi Shen, Tian-ru Xiao, Yan-cheng Li. "Quantum Pattern Search with Closed Match", International Journal of Theoretical Physics, 2013 Publication	<1 %
20	www.cl.cam.ac.uk Internet Source	<1 %
21	www.tandfonline.com Internet Source	<1 %
22	Hari P. Paudel, Madhava Syamlal, Scott E. Crawford, Yueh-Lin Lee et al. "Quantum Computing and Simulations for Energy Applications: Review and Perspective", ACS Engineering Au, 2022 Publication	<1 %
23	Sina Shokri, Shahnoosh Rafibakhsh, Roghayeh Pooshgan, Rita Faeghi. "Implementation of a	<1 %

quantum algorithm to estimate the energy of a particle in a finite square well potential on IBM quantum computer", The European Physical Journal Plus, 2021

Publication

-
- | | | |
|----|---|------|
| 24 | lib.unisayogya.ac.id
Internet Source | <1 % |
|----|---|------|
-
- | | | |
|----|---|------|
| 25 | publik.tuwien.ac.at
Internet Source | <1 % |
|----|---|------|
-
- | | | |
|----|--|------|
| 26 | Michael Kühn, Sebastian Zanker, Peter Deglmann, Michael Marthaler, Horst Weiß.
"Accuracy and Resource Estimations for Quantum Chemistry on a Near-Term Quantum Computer", Journal of Chemical Theory and Computation, 2019
Publication | <1 % |
|----|--|------|
-
- | | | |
|----|---|------|
| 27 | Natalie Klco, Alessandro Roggero, Martin J Savage. "Standard Model Physics and the Digital Quantum Revolution: Thoughts about the Interface", Reports on Progress in Physics, 2022
Publication | <1 % |
|----|---|------|
-
- | | | |
|----|---|------|
| 28 | citeseerx.ist.psu.edu
Internet Source | <1 % |
|----|---|------|
-
- | | | |
|----|---|------|
| 29 | epdf.pub
Internet Source | <1 % |
|----|---|------|
-

30 J.S. Popovics, J.L. Rose. "An approach for wave velocity measurement in solid cylindrical rods subjected to elastic impact", International Journal of Solids and Structures, 1996 <1 %
Publication

31 Santanu Pattanayak. "Quantum Machine Learning with Python", Springer Science and Business Media LLC, 2021 <1 %
Publication

Exclude quotes On

Exclude matches Off

Exclude bibliography On